City Research Online

City, University of London Institutional Repository

Citation: Read, M. G., Stosic, N. & Smith, I. K. (2017). Operational characteristics of internally geared positive displacement screw machines. In: ASME 2017 International Mechanical Engineering Congress and Exposition. . USA: ASME. ISBN 9780791858417 doi: 10.1115/IMECE2017-70228

This is the accepted version of the paper.

This version of the publication may differ from the final published version.

Permanent repository link: https://openaccess.city.ac.uk/id/eprint/19410/

Link to published version: https://doi.org/10.1115/IMECE2017-70228

Copyright: City Research Online aims to make research outputs of City, University of London available to a wider audience. Copyright and Moral Rights remain with the author(s) and/or copyright holders. URLs from City Research Online may be freely distributed and linked to.

Reuse: Copies of full items can be used for personal research or study, educational, or not-for-profit purposes without prior permission or charge. Provided that the authors, title and full bibliographic details are credited, a hyperlink and/or URL is given for the original metadata page and the content is not changed in any way.

City Research Online: http://openaccess.city.ac.uk/ publications@city.ac.uk

Operational Characteristics of Internally Geared Positive Displacement Screw Machines

Matthew Read, Nikola Stosic and Ian K Smith
Centre for Compressor Technology
Department of Mechanical
Engineering & Aeronautics
City, University of London
London, EC1V 0HB, UK
Email: m.read@city.ac.uk

Abstract

Cylindrical helical gearing profiles can allow an externally lobed inner gear to rotate inside an internally lobed outer gear while maintaining continuous lines of contact between the gears. A series of separate working chambers are formed between the rotors, and this paper investigates the use of ported end plates to control the period during which fluid is allowed to enter or leave these working chambers. A simple method of defining the rotor profiles is considered, allowing the geometry of such internally geared screw machines to be characterised. The performance of the machine is then investigated for particular applications. The key considerations in this preliminary study are the effect of geometry on the forces and torques that act on both the inner and outer rotors. The results suggest that low rotor contact forces are possible, which is necessary to ensure high efficiency and low wear in practical machines.

Nomenclature

p	Pressure (bar)
L	Rotor length (m)
V	Volume (m^3)
T	Torque (Nm)
r	Profile radius (m)
A	Area (m^2)
ρ	Diameter (m)
E	Distance between rotor axes (m)
N	Number of lobes on rotor

P	Power (W)
W_{cyc}	Work done per cycle (J)
ω	Angular speed (rad/s)
θ	Cycloid generating angle (rad)
ϕ_w	Wrap angle of rotor (rad)
ϵ_v	Built-in volume ratio

Introduction

Conventional twin screw machines consist of two externally lobed helical rotors, which rotate about parallel axes within a fixed casing. The rotors are carefully shaped to ensure that lines of continuous contact occur between the rotors. This combined with the small clearance gap between the rotor tips and the casing creates a series of separate working chambers. The volume of a working chamber enclosed within the two rotors and the side and end faces of the casing is seen to vary with the angular position of the rotors. Carefully shaped holes, or ports, in the end faces of the casing then allow fluid to enter and leave the working chambers once specified volumes are reached, allowing either compression or expansion of the fluid passing through the machine. Internally geared rotors are used in various configurations of pump, either as straight cut rotors (such as Gerotor or internal lobe pumps) or as helical rotors with open ends. An important feature of the rotor profiles is the requirement for continuous contact between rotors. Details of rotor profile generation for such applications are described by an number of authors [1–5]. In a patent from 1932, Moineau [6] describes some simple methods of defining rotor geometry for these applications while also proposing the use of rotors with variable pitch or variable profile in order to achieve a change in the volume of the working chamber between inlet and discharge of the machine. More recent developments have looked at implementing the concept of conical internally geared rotors for a range of compressor applications [7]. There are however challenges in manufacturing rotors of this geometry at reasonable cost and with the accuracy required for efficient operation.

Internally geared rotors with porting

In order to simplify the manufacture of internally geared screw machines, a novel configuration is proposed by the authors in which the rotors have constant pitch and profile. Both rotors are allowed to rotate about fixed parallel axes. An example of this arrangement is shown in Figure 1, and details of the required rotor geometry are discussion in the following section. With open ends, this configuration functions as a pump. However, the use of fixed end plates with porting allows control over the periods during which fluid can enter and leave the working chamber. By closing the working chamber from both end of the machine while the volume is varying, the machine can therefore operate as either a compressor or expander. An example of the shape of the port required at the high pressure end face of the machine is shown in Figure 2. In the rotor positions shown in Figure 2 it can be seen that several working chamber are exposed to the high pressure end face, but fluid cannot leave the compressor until exposed to the port opening. An advantage of using end plates with constant pitch and profile helical rotors is that it can potentially reduce the manufacturing complexity compared to the variable pitch and/or profile configuration; the inner rotor can be manufactured with high precision using the same methods as conventional twin screw rotors, while the outer rotors can potentially be made using internal grinding methods.

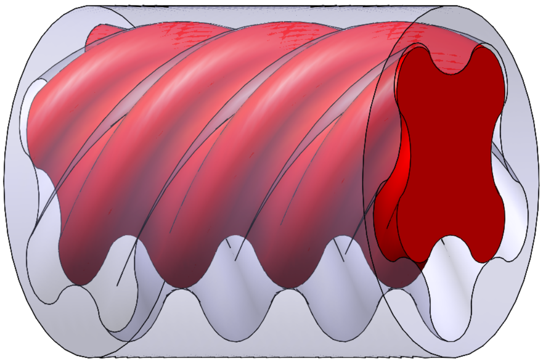

Figure 1: Example of the internally geared screw machine rotors with $N_i = 4$.

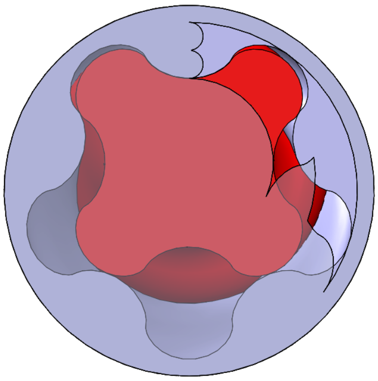

Figure 2: Example of a ported end-plate at the high pressure end of the internally geared screw machine with $N_i = 4$.

Geometry of simple rotor profiles for internally geared machines

Internally geared positive displacement machines require continuous contact points between inner and outer rotors during rotation about parallel axes. This allows the formation of enclosed working chambers whose volume varies with the angular position of the rotors. A wide range of rotor profiles can be generated that meet this requirement. In this paper, simple geometries consisting of epicycloids and hypocycloids are used to illustrate this requirement of continuous contact between rotors and to investigate machine performance. These profiles require that the inner rotor has one fewer lobe than the outer rotor. The equations defining coordinates of epicycloid and hypocycloid profiles are shown in Equations 1 and 2. While cycloids are used in this paper to illustrate the analysis of internally geared machines, it should be noted that there is considerable scope for optimisation using other methods of rotor profile generation.

$$\begin{bmatrix} x_e(\theta) \\ y_e(\theta) \end{bmatrix} = \begin{bmatrix} (\rho_b + \rho_e)cos(\theta) - \rho_e cos(\theta(\rho_b/\rho_e + 1)) \\ (\rho_b + \rho_e)sin(\theta) - \rho_e sin(\theta(\rho_b/\rho_e + 1)) \end{bmatrix} \tag{1}$$

$$\begin{bmatrix} x_h(\theta) \\ y_h(\theta) \end{bmatrix} = \begin{bmatrix} (\rho_b - \rho_h)cos(\theta) + \rho_h cos(\theta(\rho_b/\rho_h - 1)) \\ (\rho_b - \rho_h)sin(\theta) - \rho_h sin(\theta(\rho_b/\rho_h - 1)) \end{bmatrix} \tag{2}$$

Continuous contact between rotors can be achieved using composite profiles which can be created by combining sections of epicycloid and hypocycloid profiles. The profiles are defined by the radius of the base circle, ρ_b, the number of lobes required on the rotor, N, and the radius of the epicycloid generating circle, ρ_e, where $0 \leq \rho_e \leq \rho_b/N$. By considering the circumferences of the epicycloid and hypocycloid generating circles, it can be seen that the radius of the hypocycloid generating circle is:

$$\rho_h = \rho_b/N - \rho_e \tag{3}$$

The maximum and minimum radii of the rotor are as follows:

$$\rho_{max} = \rho_b + 2\rho_e, \quad \rho_{min} = \rho_b - 2\rho_h \tag{4}$$

It is clear that when $\rho_e = 0$ or $\rho_h = 0$, the rotor is a pure hypocycloid or epicycloid respectively. In order to achieve the required meshing condition between the inner and outer rotors it can be shown ρ_e and ρ_h must be equal for both rotors and that:

$$\rho_{e,o}/E = \rho_{e,o}/(\rho_{e,o} + \rho_{h,o}) \tag{5}$$

It can be seen from Equation 5 that the possible values of the ratio ρ_e/E range between zero and one, corresponding to the cases when the rotors are pure hypocycloids and epicycloids respectively. Examples of different rotor profiles are shown in Figure 3. In all the examples presented in this paper, the geometric parameters for the outer rotor have been chosen in order to achieve a maximum profile radius, $r_{o,max}$, of 0.5 m, and the profiles are therefore bounded by a circle of diameter 1 m.

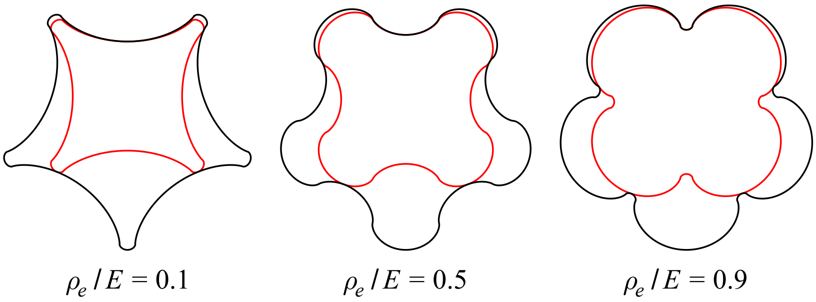

Figure 3: Effect of ρ_e/E on rotor geometry with $N_i = 4$

Geometric characteristic of internally geared machines

Once the rotor profiles have been specified the contact points can be identified using the meshing condition for the two rotors. This states that the normal to the surface of both rotors at a point of contact must pass through the pitch point of the rotors, which is the point where the base circles of the inner and outer rotors coincide. The area contained between two rotor contact points can then be characterised as a function of the angular position of the rotor profiles. This working chamber area is seen to increase from zero (at the angular position where two contact points converge) to a maximum value, as shown in Figure 3. Due to the symmetry of the rotor lobes, the relationship of the working chamber area with the angular position is symmetrical about this point of maximum area.

For helical rotors at a fixed angular position, the variation of area with profile angular position can be related to the cross-sectional area of the working chamber as a function of longitudinal location. As for conventional screw machines, this requires the wrap angle of the rotors, $\phi_{w,o}$, to be defined along with the rotor length [8]. The values used for the analysis presented in this paper are specified in Table 1. Hence, for a specific rotor position, the volume of the working chamber can be found by performing an integration of the area w.r.t. the longitudinal coordinate, z. The working chamber volume can therefore be found as a function of rotor position. The swept volume per revolution of a rotor is then equal to the maximum working chamber volume multiplied by the number of lobes on the rotor, N, as shown in Equation 6. The resulting value of swept volume is shown in Figure 4 for $0 < \rho_e/E < 1$ and for a range of values of N_i.

$$v_{sw} = v_{wc,max} \times N \tag{6}$$

Table 1: Characteristics of internal screw geometry.

Parameter	Value
Outer rotor length-diameter ratio, $L/2r_{o,max}$	1.55
Outer rotor wrap angle, $\phi_{o,w}$	300°

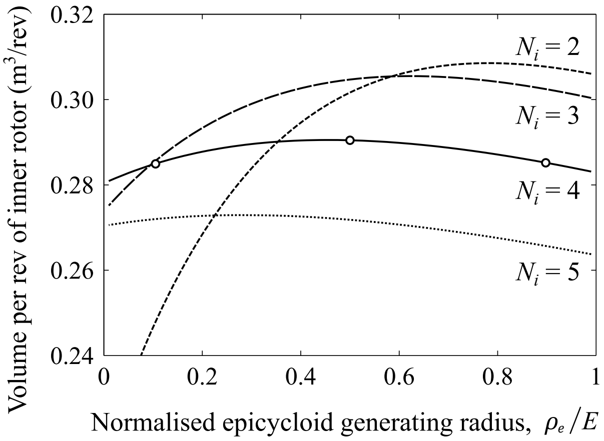

Figure 4: Swept volume of internally geared machines with simple composite epi-hypo cycloid profiles

The results in Figure 4 suggest that for the simple composite cycloid profiles considered here, the value of ρ_e/E does not have a large effect on the swept volume for cases with $N_i > 2$. For $N_i = 3$ the difference between the maximum and minimum swept volume is seen to be less than 10%, and this decreases as N_i increases; for $N_i = 4$ the minimum is less than 2% smaller than the maximum which occurs at $\rho_e/E \approx 0.5$. Increasing N_i is seen to reduce the maximum possible swept volume, but there is clearly significant scope for optimising the overall performance of internally geared machines by varying both lobes number and profile. Once the volume of the working chamber has been characterised as a function of rotor position, the performance of the machine can be investigated for particular applications. The key considerations in this analysis are the effect of geometry on the forces and torques that act on both the inner and outer rotors.

Built-in volume ratio of machine

The built-in volume ratio (ϵ_v) of the machine is the ratio of the maximum working chamber volume to the minimum volume at which the working chamber remains closed from either the suction or discharge ports. The volume vs. rotor position curve allows the geometry of the suction and discharge ports to be defined in order to achieve a particular value of ϵ_v. This is achieved by identifying the position of the rotor profiles at the high pressure end face of the rotors at the point where the working chamber volume reaches the required value. These profiles are then used along with the loci of contact points to define a port area which ensures that flow can only enter or leave the working chamber once the required position is reached, as discussed in the following section.

Port geometry and resulting flow areas

An example of port geometry generation is illustrated using 4 lobe internal and 5 lobe external configuration with L/D = 1.55, wrap angle = 300°. Construction of maximum port area for high pressure port requires the following:

1. Rotor contact locus projected onto high pressure end face
2. Circle with minimum inner rotor diameter centred on inner rotor axis
3. Circle with maximum outer rotor diameter centred on outer rotor axis
4. Inner and outer rotor profiles at high pressure end face with angular position corresponding to volume of working chamber, $v_{wc} = v_{max}/\epsilon_v$

This is illustrated in Figure 5 for the case when $\epsilon_v = 4.5$. A similar construction method is used to find the maximum port area for the low pressure port, using the rotor-to-rotor contact line projected onto low pressure end face, circle with minimum inner rotor diameter centred on inner rotor axis and circle with maximum outer rotor diameter centred on outer rotor axis. The inner and outer rotor profiles at low pressure end face with angular position corresponding to volume of working chamber $v_{wc} = v_{max}$, then define the port shape as shown in Figure 6.

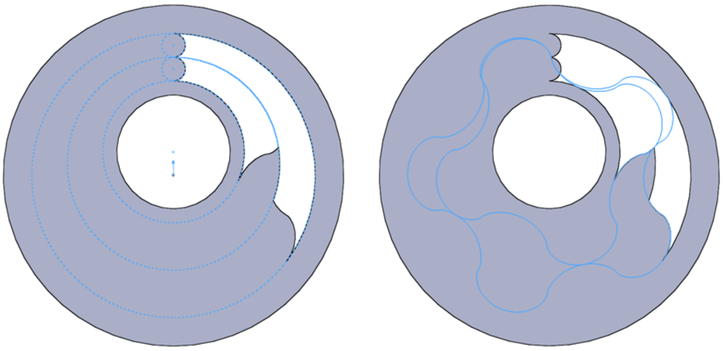

Figure 5: Construction of high pressure port geometry with $N_i = 4$, $\rho_e/E = 0.5$, $\phi_{w,o} = 300°$, $L/D = 1.55$ and $\epsilon_v = 5$

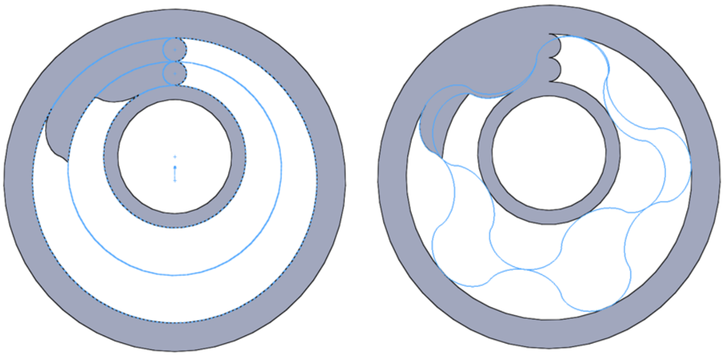

Figure 6: Construction of low pressure port geometry with $N_i = 4$, $\rho_e/E = 0.5$, $\phi_{w,o} = 300°$, $L/D = 1.55$

If the wrap angle is sufficient to create a working chamber that is completely enclosed by rotor-to-rotor contact lines, then the discharge end face can be completely open without affecting the maximum volume of low pressure fluid in the machine. Even if this is not the case, a completely open discharge port can still be used, but this results in a reduced maximum volume (and hence ϵ_v if the same high pressure port is used); this may be preferable for simplifying the placement and design of components such as timing gears and rotor bearings. Once the port areas have been defined the flow area can be calculated as a function of the rotor positions. This has been calculated using CAD software to assess the overlapping regions between the area of the working chamber on the relevant end face and the area of the port opening. This can be seen in Figure 7, where two working chambers are exposed to the high pressure port at the rotor position shown; the flow area of working chamber with the larger volume is shown in light green and consists of two discrete openings separated by part of the port, while the smaller working chamber has a single opening shown in dark green. These flow areas are calculated as a function of outer rotor position, and the total low and high pressure flow areas for a particular working chamber are shown in Figure 8 for the case when $\rho_e/E = 0.5$. The dashed red line in Figure 8 illustrates the area of the working chamber exposed to the high pressure end face, and therefore represents an upper limit to the flow area at the high pressure port. A comparison of the high pressure flow areas for the three cases when $\rho_e/E = 0.1$, 0.5 and 0.9 is shown in Figure 9.

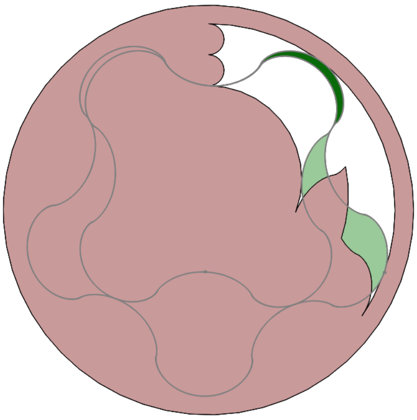

Figure 7: Example of the working chamber flow areas at the high pressure port

The results in Figure 9 shown that of the three cases, the maximum flow area for the high pressure port occurs when $\rho_e/E = 0.5$. As can be seen from Figure 4 this is also very close to the maximum swept volume for the specified maximum rotor profile radius of 0.5m. Increasing or decreasing the value of ρ_e/E to 0.9 or 0.1 respectively is seen to significantly decrease the maximum flow area while only slightly reducing the swept volume. This is likely to influence the pressure of the working fluid during the discharge process for a compressor (or filling process for an expander). A more important consideration, however, is the effect that the choice of profile has on the pressure forces and resulting torque acting on both the inner and outer rotors. This is discussed in the following section.

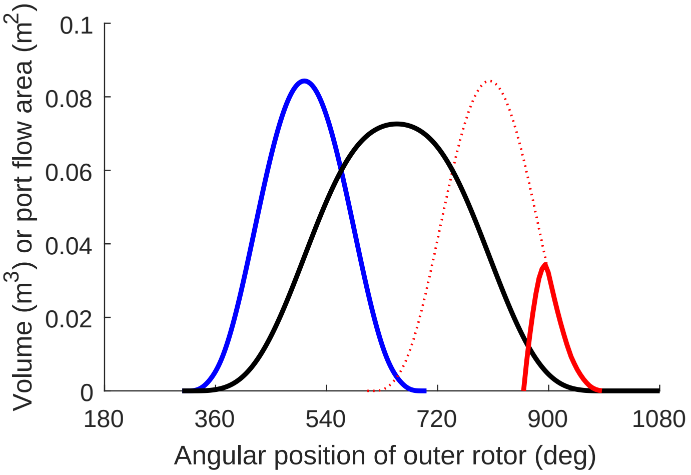

Figure 8: Working chamber volume (black line), LP port flow area (blue line) and HP port flow area (red line) for $N_i = 4$, $\rho_e/E = 0.5$, $\phi_{w,o} = 300°$, $L/D = 1.55$

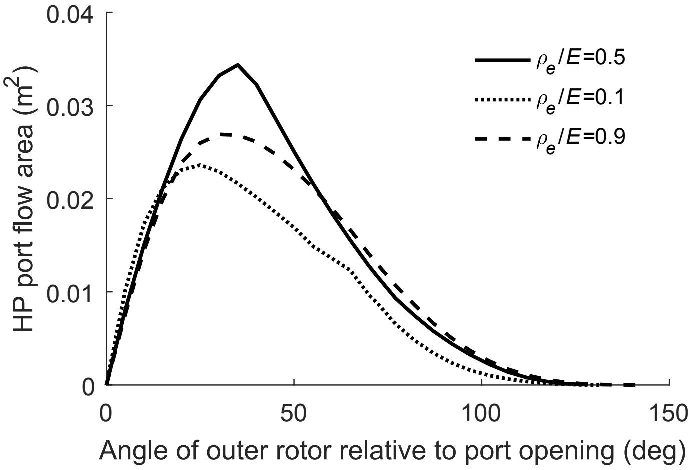

Figure 9: HP port flow area for a range of ρ_e/E with $N_i = 4$, $\theta_{w,o} = 300°$, $L/D = 1.55$

Operational characteristic of internally geared machines

In order to investigate the operation of internally geared machines a number of assumption shave been made. The working fluid is assumed to be an ideal gas with $\gamma = 1.4$, and the compression process is assumed to isentropic. The discharge pressure from the compressor is assumed to be equal to working chamber pressure after compression process (i.e. there is no over or under compression), and the pressure is assumed to remain constant during filling and discharge of working chamber. Leakage between the inner and outer rotors or between end plates and rotor end faces has also been neglected.

Radial force and torque on rotors

The assumptions described above allow a simple investigation of the effects of rotor geometry, as radial forces and rotor torques can be derived from integration along the z axis (the longitudinal coordinate) of pressure acting on the projected area between rotor contact points. At a particular longitudinal position, the contact points between the rotors can be used to find the projected length over which the pressure is acting in the x-y plane of the rotors. The resultant pressure force per unit length can be considered to act at the centre of this line and in a direction perpendicular to it. The torque arm distances between the line of action of the pressure force and the rotational axes of the two rotors can then be found. It is clear that the radial force on the two rotors must be of equal magnitude and opposite in direction. This force multiplied by the torque arm distances gives the rotor torques per unit length, which can then be integrated along the z coordinate to find the net torque acting on each rotor. It is possible to check the net torque for these profiles by calculating the work done per revolution of the outer rotor for the isentropic process with the average torques of the two rotors, as shown in Equations 7 and 8:

$$W_{cyc} = (\gamma/(\gamma - 1))[P_{dis}(V_{max}/\epsilon_v) - P_{suc}V_{max}] \tag{7}$$

$$P = W_{cyc}N_o\omega_o/2\pi = \omega_o[\bar{T}_o + \bar{T}_i(N_o/N_i)] \tag{8}$$

where $\bar{T}$ is the time averaged value of the rotor torque (assuming constant rotational speed). In all cases presented here, the torque values calculated using the numerical integration described are found to agree with the calculated work done to within 0.1%.

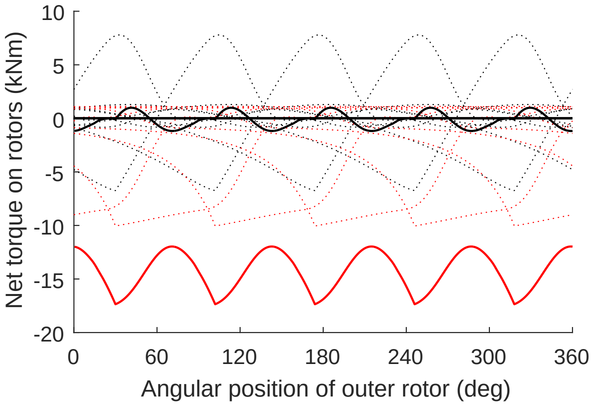

Figure 10: Net torque on outer (black) and inner *red) rotors with $\rho_e/E = 0.1$, $N_i = 4$, $\phi_{w,o} = 300°$, $L/D = 1.55$ and $\epsilon_v = 5$

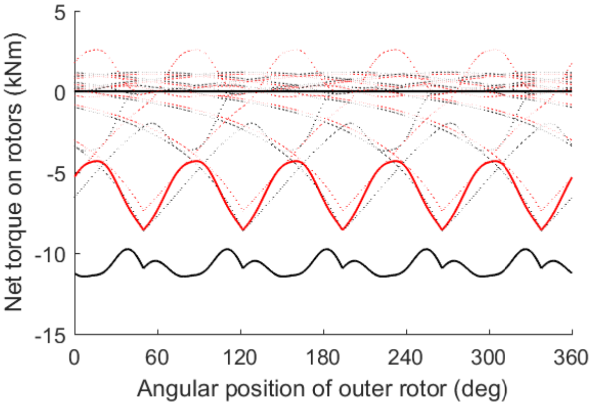

Figure 11: Net torque on outer (black) and inner *red) rotors with $\rho_e/E = 0.5$, $N_i = 4$, $\phi_{w,o} = 300°$, $L/D = 1.55$ and $\epsilon_v = 5$

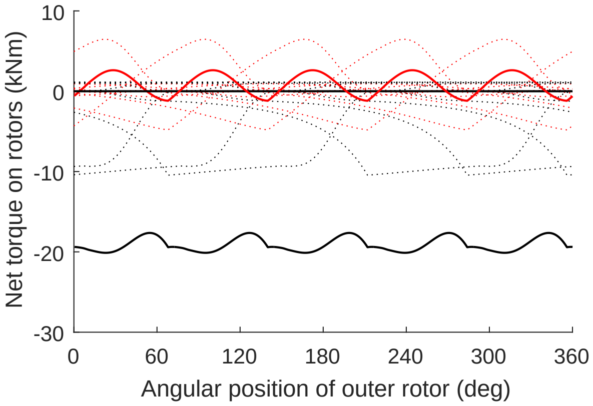

Figure 12: Net torque on outer (black) and inner *red) rotors with $\rho_e/E = 0.9$, $N_i = 4$, $\phi_{w,o} = 300°$, $L/D = 1.55$ and $\epsilon_v = 5$

The three examples shown in Figures 10-12 illustrate the importance of rotor profile on the operation of the internally geared machine. It is clear that for a compressor, the rotor with the largest time averaged torque should be the driven rotor as this will mean that more of the shaft power driving the compressor is delivered directly to the fluid, and the power transmission between the rotors will be reduced. This ratio of undriven-to-driven rotor torques is shown for the three cases in Figure 13. It is clear that using either a high or low value of ρ_e/E can result in low contact forces between the rotors; when ρ_e/E is close to zero the inner rotor should be driven in order to minimise power transmission to the outer rotor, while for values of ρ_e/E closer to 1 the outer rotor should be driven.

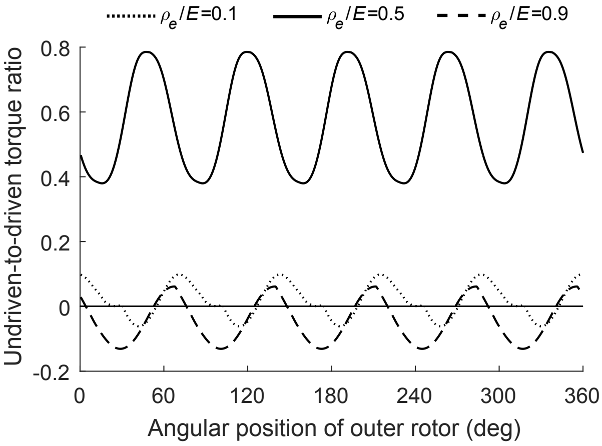

Figure 13: Ratio of undriven-to-driven rotor torques when chosen to minimise contact forces for the cases shown in Figures 10-12

Effect of compression process on rotor torque ratio

A simple sensitivity analysis has been performed in order to investigate the effect of the compression process on the ratio of torques in the undriven and driven rotors. For the case with $\rho_e/E = 0.1$ (see Figure 10) the polytropic exponent has been varied from the isentropic case of $n = \gamma$ (1.4 for air, as used in the previous calculations) to the case when $n = 1$ corresponding to isothermal compression. The results are shown in Figure 14 and indicate that although the effect of varying n is relatively small, the details of the compression process should be considered when specifying rotor profiles to minimise this torque ratio, especially in applications with oil injection where heat transfer will be significant.

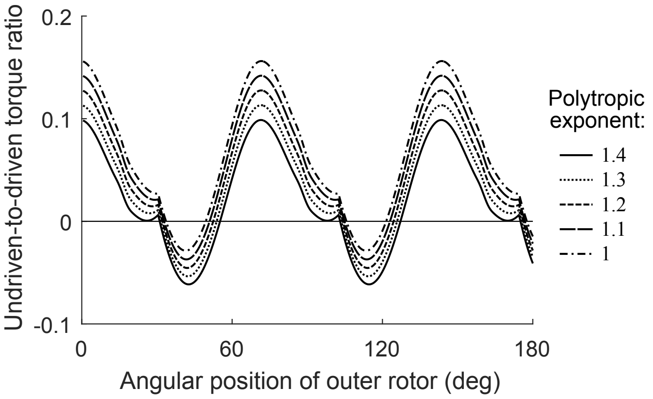

Figure 14: Effect of polytropic exponent when $\rho_e/E = 0.1$

Comparison with conventional screw machine geometry

The results for the internally geared screw machine presented above can be compared with a conventional screw machine. To provide a basis for comparison, geometry data for a conventional 102mm oil-injected screw compressor has been used with $\epsilon_v = 5$, and with 4 & 5 lobes on the main and gate rotors respectively. This data has been calculated using software developed at City, University of London based on the analysis methods described by Stosic et al. [8]. This conventional screw machines has the geometric properties shown in Table 2. The internally geared profiles with $\rho_e/E = 0.1$, 0.5 and 0.9 have been used to provide an initial comparison between the two configurations, and the geometry of the rotors has been scaled in order to achieve the same swept volume per revolution of the 4-lobed rotor. The maximum profile radius of the rotor with N lobes, $r_{N,max}$ is given in Table 2 for all cases, along with the rotor lengths, and the maximum axial flow areas for the high and low pressure ports, $A_{hp,max}$ and $A_{lp,max}$.

While the same value of $L/D = 1.55$ has been used for both the conventional and internally geared machines it has been applied to the rotor with the largest profile diameter in each case. Therefore, in order to match the swept volume of the conventional machine, the maximum diameter and length of the internally geared machines are around 35% larger for all three values of ρ_e/E. The largest axial port areas are achieved when $\rho_e/E = 0.5$. When compared to the conventional machine, the axial high and low pressure port flow areas for this case are 48% and 45% larger respectively. However, this case will have high power transfer between the rotors. The case with $\rho_e/E = 0.1$ (when the inner rotor should be driven in order to minimise power transmission to the outer rotor) achieves a very similar high pressure port area to the conventional machine, but has a 32% larger axial low pressure port area. It should be noted however that radial ports are not possible for the internally geared configuration. For the conventional machine considered here with $\epsilon_v = 5$ no radial port is possible at the high pressure end due to geometrical constraints, but a large radial port area is possible at the low pressure end, resulting in a total port area of around 10 times the values of $A_{lp,max}$ shown in Table 2 for the internally geared machines.

It is clear that there is considerable scope to optimise the geometry of the internally geared machines in order to achieve a compromise between high swept volume, low power transmission between gears and low pressure loss during filling and discharge of the working chamber. This will require a more rigorous investigation of the complex flows through the high and low pressure ports and the effects of leakage between working chambers. The significantly lower sliding velocities that occur between the rotors in the internally geared configuration are expected to allow higher rotational speeds to be achieved than are possible in a conventional machines, which will also need to be considered during design optimisation.

Table 2: Comparison of conventional and internally geared screw machines with equal volume per revolution.

Parameter	Conv.		Int.	
ρ_e/E	-	0.5	0.1	0.9
v_{sw} (l/rev)	0.716	-	-	-
$r_{4,max}$ (mm)	101.9	109.8	112.6	115.9
$r_{5,max}$ (mm)	80.2	136.0	135.1	135.9
Length (mm)	158.0	210.8	209.4	210.7
$A_{hp,max}$ (mm^2)	428	635	431	497
$A_{lp,max}$ (mm^2)	1163	1681	1539	1434

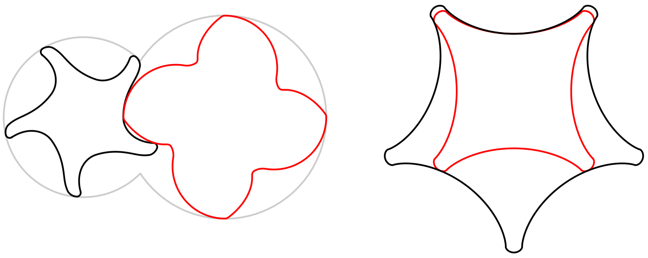

Figure 15: Rotor geometry for conventional and internally geared rotors ($\rho_e/E = 0.1$) when scaled for equal swept volume as shown in Table 2

Conclusions

The analysis presented in this paper illustrates the characteristics of a novel internally geared positive displacement machine consisting of constant pitch and profile rotors rotating about fixed, parallel axes. Examples of simple cycloidal rotor profiles that meet the requirement of continuous contact between rotors have been described, and the stationary end face porting required to achieve compression or expansion of fluid in such a device has been discussed. The maximum area of axial high pressure ports have been defined for a specified built-in volume ratio, and the variation of flow area with rotor position has been calculated. A simple isentropic ideal gas compression model has been used to investigate the torques exerted on the rotors, leading to the following conclusions:

For the simple composite cycloidal profiles consider in this paper, the time averaged torque on the inner or outer rotor can be minimized by selection of the value of ρ_e/E.

When $N_i > 2$, the value of ρ_e/E has little effect on the swept volume of the machine for a given rotor diameter, length and wrap angle.

When $N_i = 4$ the maximum swept volume and high pressure port area occur when $\rho_e/E \approx 0.5$, but the power transfer between rotors is minimised when $\rho_e/E \approx 0.1$ or 0.9 depending on whether the inner or outer rotor should be driven. The maximum flow area at the high pressure port is significantly reduced for cases where the power transmission between rotors is minimised.

The size of the internally geared machines is roughly comparable to a conventional screw machine with the same swept volume. However, more work is required to assess the affect of rotor geometry, port geometry and operating speed on the performance of internally geared machines in order to optimise the design for specific applications.

References

[1] Colbourne, J.R., 1974. The geometry of trochoid envelopes and their application in rotary pumps. Mechanism and Machine Theory, 9(3-4), pp.421-435.

[2] Beard, J.E., 1985. Kinematic analysis of gerotor type pumps, engines, and compressors, PhD thesis.

[3] Beard, J.E., Yannitell, D.W. and Pennock, G.R., 1992. The effects of the generating pin size and placement on the curvature and displacement of epitrochoidal gerotors. Mechanism and Machine Theory, 27(4), pp.373-389.

[4] Vecchiato, D., Demenego, A., Argyris, J. and Litvin, F.L., 2001. Geometry of a cycloidal pump. Computer methods in applied mechanics and engineering, 190(18), pp.2309-2330.

[5] Litvin, F.L. and Fuentes, A., 2004. Gear geometry and applied theory. Cambridge University Press.

[6] Moineau, R.J.L., 1932. Gear mechanism. U.S. Patent 1,892,217.

[7] Dmitriev, O., Tabota, E., and Arbon, I., 2015. A miniature Rotary Compressor with a 1:10 compression ratio. IOP Conference Series: Materials Science and Engineering. Vol. 90. No. 1. IOP Publishing.

[8] Stosic, N., Smith, I. and Kovacevic, A., 2005. Screw compressors: mathematical modelling and performance calculation. Springer Science & Business Media.